Förster resonance energy transfer, absorption and emission spectra in multichromophoric systems. II. Hybrid cumulant expansion

Citation: Ma, Jian; Moix, Jeremy and Cao, Jianshu. "Förster Resonance Energy Transfer, Absorption and Emission Spectra in Multichromophoric Systems. II. Hybrid Cumulant Expansion." Journal of Chemical Physics 142, 9 (March 2015): 094107 © 2015 AIP Publishing LLC

As Published: http://dx.doi.org/10.1063/1.4908600

Publisher: American Institute of Physics (AIP)

Persistent URL: http://hdl.handle.net/1721.1/110442

Version: Final published version: final published article, as it appeared in a journal, conference proceedings, or other formally published context

Förster resonance energy transfer, absorption and emission spectra in multichromophoric systems. II. Hybrid cumulant expansion

Jian Ma, Jeremy Moix, and Jianshu Cao

Citation: The Journal of Chemical Physics **142**, 094107 (2015); doi: 10.1063/1.4908600
View online: http://dx.doi.org/10.1063/1.4908600
View Table of Contents: http://scitation.aip.org/content/aip/journal/jcp/142/9?ver=pdfcov
Published by the AIP Publishing

Förster resonance energy transfer, absorption and emission spectra in multichromophoric systems. II. Hybrid cumulant expansion

Jian Ma, Jeremy Moix, and Jianshu Cao[a)]
Department of Chemistry, Massachusetts Institute of Technology, Cambridge, Massachusetts 02139, USA

(Received 13 August 2014; accepted 6 February 2015; published online 3 March 2015)

We develop a hybrid cumulant expansion method to account for the system-bath entanglement in the emission spectrum in the multi-chromophoric Förster transfer rate. In traditional perturbative treatments, the emission spectrum is usually expanded with respect to the system-bath coupling term in both real and imaginary time. This perturbative treatment gives a reliable absorption spectrum, where the bath is Gaussian and only the real-time expansion is involved. For the emission spectrum, the initial state is an entangled state of the system plus bath. Traditional perturbative methods are problematic when the excitations are delocalized and the energy gap is larger than the thermal energy, since the second-order expansion cannot predict the displacement of the bath. In the present method, the real-time dynamics is carried out by using the 2nd-order cumulant expansion method, while the displacement of the bath is treated more accurately by utilizing the exact reduced density matrix of the system. In a sense, the hybrid cumulant expansion is based on a generalized version of linear response theory with entangled initial states. © *2015 AIP Publishing LLC.* [http://dx.doi.org/10.1063/1.4908600]

I. INTRODUCTION

In the study of excitonic energy transfer (EET),[1] if a system has two well distinguished parts, usually termed as the donor and acceptor, then the EET rate between them is given by the Förster resonance energy transfer (FRET) rate[1] when both the donor and acceptor are monomers, i.e., point dipoles.

However, the FRET theory is invalid in complex systems where the donor and acceptor have multiple chromophores. Therefore, a multi-chromophoric Förster transfer (MCFT) theory was developed.[2] In the framework of the MCFT theory, the EET process is described as follows: first, the donor is excited to its single-excitation subspace, and then relaxes to its single-excitation equilibrium state on an ultrafast time-scale. We should note that this state is the entangled equilibrium state of the donor and its bath together. After that, the excitonic energy of the donor can either be emitted to the environment radiatively or transferred to the acceptor non-radiatively through dipole-dipole couplings. This non-radiative process is the MCFT. In most cases, the radiative lifetimes are much longer than the non-radiative MCFT lifetimes, and can be neglected within the EET process.

The MCFT rate can be derived via Fermi's golden rule, and is given by the product of the square of the donor-acceptor coupling, and the overlap integral of the donor's emission and acceptor's absorption spectra tensors. We should note that the spectra tensors in the MCFT rate are different from the standard far-field spectra. The MCFT rate can be obtained exactly from numerical methods such as hierarchy equation of motion (HEOM)[3,4] and our recently developed stochastic path integrals (PI).[5,6] However, realistic systems are so large that the exact numerical methods cannot be applied, and thus we need to use perturbative methods such as the full 2nd-order cumulant expansion (FCE),[7] 2nd-order time-convolution (TC2), and time-convolution-less (TCL2)[8–10] equations.

Both the absorption and emission spectra are the Fourier transforms of the time-correlation functions of the dipole operators. For the absorption spectrum, the dipole operators are averaged over the equilibrium distribution of the acceptor's free bath ρ_b^A, which is modeled by a set of oscillators and obeys Gaussian statistics. In the calculation of the absorption spectrum, no population dynamics is involved, and the coherence decays so fast that the FCE method can give reliable results. However, in the emission spectrum, the dipole operators are averaged with respect to ρ_e^D, which is the equilibrium state of the donor's excitons and its bath. The FCE and other 2nd-order methods such as TCL2[10] are not reliable due to the system-bath entanglement.

In the special case that the donor is a monomer, the system-bath coupling results in a scalar displacement in the bath, which can be removed by the polaron transformation,[11–13] and the emission spectrum can be obtained exactly by using the FCE. However, if the donor has multiple chromophores and its free excitations are highly delocalized, the displacements of the bath are not scalars but matrices and the polaron transform cannot be applied. In this case, traditional 2nd-order perturbative methods such as the FCE and TC2 can work only for high temperatures, since the coherence in the donor is strongly suppressed by thermal fluctuations and the excitations are essentially localized. Usually, the temperatures of real systems are not high as compared with inter-chromophoric couplings. For example,

a)Electronic address: jianshu@mit.edu

in LH2 the thermal energy at $T = 300$ K is of the same order as the inter-chromophoric coupling and the reorganization energy.

To overcome this problem, we develop a new perturbative method to calculate the displacements of the bath from the exact reduced density matrix (RDM) of the donor, which is obtained numerically exactly via imaginary-time path integrals.[6] In the high-temperature limit, the new method reduces to our full cumulant expansion. The improvement of the emission spectrum is shown in Sec. III A. We note that the HEOM method can give the exact displacements from its auxiliary fields,[14] but it is too numerically expensive even for LH2 and the spectral density of the system-bath coupling is restricted to be of Drude-Lorentz form. For these reasons, we have developed stochastic path integrals[15] which apply to large systems with any spectral densities. A systematic comparison of different methods for the LH2 complex will be presented in our Paper IV,[6] where the benchmark emission spectrum and MCFT rate are obtained with our stochastic PI method.

This paper is organized as follows. In Sec. II, we first introduce the MCFT theory and the absorption and emission spectra. In Sec. II B, we derive the emission spectrum by combining the cumulant expansion method with the exact reduced density matrix of the donor. Then, we present numerical results and comparisons in Sec. III A.

II. THEORY

A. Model Hamiltonian and multi-chromophoric theory

Most of this subsection can be found in our Paper I.[7] Here, for the sake of completeness, we give a brief introduction of the model and theory.

To define the MCFT rate, we first model the multi-chromophoric system. The total Hamiltonian is

$$H = H^D + H^A + H_c, \tag{1}$$

where $H^{D(A)}$ is the Hamiltonian of the donor (acceptor) and its bath. H_c is the dipole-dipole coupling between the donor and the acceptor. For the donor's part,

$$H^D = H_s^D + H_b^D + H_{sb}^D, \tag{2}$$

where H_s^D is the donor's free Hamiltonian. In the above Hamiltonian, we do not include the degrees of freedom of the bath that are coupled with the acceptor. If the donor has N_D chromophores, its Hamiltonian in the single-excitation site basis $|D_m\rangle$ is

$$H_s^D = \sum_{m=1}^{N_D} \left(\epsilon_m^D + \lambda_m^D\right) |D_m\rangle\langle D_m| + \sum_{m\neq n}^{N_D} V_{mn}^D |D_m\rangle\langle D_n|, \tag{3}$$

where ϵ_m^D is the single-excitation energy of the site m, and λ_m^D is the reorganization energy arising from the coupling between the m-site and its bath. For the sake of simplicity, we set $\lambda_m^D = \lambda$ in this work. The bath is described by a set of harmonic oscillators and couples with each chromophore independently,

$$H_b^D = \sum_{m=1}^{N_D} \sum_k \hbar\omega_{m,k}^D b_{m,k}^{D\dagger} b_{m,k}^D, \tag{4}$$

where $\omega_{m,k}^D$ is the frequency of the kth mode of the bath that associates with the mth chromophore of the donor. $b_{m,k}^{D\dagger}$ and $b_{m,k}^D$ are the bosonic creation and annihilation operators of the bath, and $[b_{m,k}^D, b_{n,l}^{D\dagger}] = \delta_{mn}\delta_{kl}$.

The excitons of the donor couple with the bath linearly as

$$H_{sb}^D = \sum_{m=1}^{N_D} B_m^D V_m^D, \tag{5}$$

where the system's operators are $V_m^D = |D_m\rangle\langle D_m|$, and the bath operators are given by

$$B_m^D = \sum_k g_{m,k}^D \left(b_{m,k}^{D\dagger} + b_{m,k}^D\right). \tag{6}$$

The system-bath coupling strength $g_{m,k}^D$ determines the reorganization energy $\lambda_m^D \equiv \sum_k \left(g_{m,k}^D\right)^2/\omega_{m,k}^D$. The acceptor's Hamiltonian can be obtained by replacing the notation D with A in the above discussion. The coupling between the donor and acceptor is

$$H_c = \sum_{m=1}^{N_D} \sum_{n=1}^{N_A} J_{mn} |D_m\rangle\langle A_n|, \tag{7}$$

where J_{mn} are the dipole-dipole couplings.

The MCFT rate can be derived from the Fermi's golden rule as[2,7]

$$k_{MC} = \frac{1}{2\pi} \int_{-\infty}^{\infty} d\omega \, \mathrm{tr}\left[\mathbf{J}^T \mathbf{E}^D(\omega) \mathbf{J} \mathbf{I}^A(\omega)\right], \tag{8}$$

where the matrix $\mathbf{J} = \sum_{m,n} J_{mn} |D_m\rangle\langle A_n|$. $\mathbf{E}^D(\omega)$ and $\mathbf{I}^A(\omega)$ are the emission and absorption operators

$$\begin{aligned} \mathbf{E}^D(\omega) &= \int_{-\infty}^{\infty} dt \, e^{-i\omega t} \mathbf{E}^D(t), \\ \mathbf{I}^A(\omega) &= \int_{-\infty}^{\infty} dt \, e^{i\omega t} \mathbf{I}^A(t), \end{aligned} \tag{9}$$

and

$$\mathbf{E}^D(t) = \mathrm{tr}_b\left(e^{iH^D t} \rho_e^D e^{-iH_b^D t}\right), \tag{10}$$

$$\mathbf{I}^A(t) = \mathrm{tr}_b\left(e^{-iH^A t} \rho_b^A e^{iH_b^A t}\right). \tag{11}$$

One can see that in the emission spectrum tensor, $\rho_e^D = \exp(-\beta H^D)/Z_e^D$ is the equilibrium state of the total system, while in the absorption spectrum $\rho_b^A = \exp(-\beta H_b^A)/Z_b^A$ is the equilibrium state of the free bath. The above equations can also be written as

$$\begin{aligned} \mathbf{E}^D(t) &= \mathrm{tr}_b\left[\hat{\mu}_D(t)\hat{\mu}_D(0)\rho_e^D\right], \\ \mathbf{I}^A(t) &= \mathrm{tr}_b\left[\hat{\mu}_A(t)\hat{\mu}_A(0)\rho_b^A\right], \end{aligned} \tag{12}$$

by using the dipole operators

$$\begin{aligned} \hat{\mu}_D &= \frac{1}{2}\sum_m (|D_m\rangle\langle 0| + |0\rangle\langle D_m|), \\ \hat{\mu}_A &= \frac{1}{2}\sum_m (|A_m\rangle\langle 0| + |0\rangle\langle A_m|), \end{aligned} \tag{13}$$

where $|0\rangle$ is the ground state. If $J_{mn} = J$, the MCFT rate can be simplified to

$$k_{MC} = \frac{J^2}{2\pi\hbar^2}\int_{-\infty}^{\infty} d\omega\, E^D(\omega)\, I^A(\omega), \tag{14}$$

where

$$\begin{aligned} E^D(\omega) &= \sum_{m',m=1}^{N_D} E^D_{m'm}(\omega), \\ I^A(\omega) &= \sum_{n',n=1}^{N_A} I^A_{n'n}(\omega). \end{aligned} \tag{15}$$

The HEOM method can give exact spectra via Eq. (12); however, even for LH2[4] the memory cost is huge. The FCE method is accurate enough for the absorption spectrum,[7] but it becomes problematic for the emission spectrum, when the donor's excitation is highly delocalized and the thermal energy is comparable to or smaller than the donor's energy gap.

B. Emission spectrum

Below, we only discuss the emission spectrum since the absorption spectrum obtained from the FCE method is sufficiently reliable. The emission spectrum is more complicated than the absorption spectrum due to the initial system-bath correlations. If the donor is a monomer or the excitations of the donor are fully localized, the displacements of the bath are scalars, which can be removed by the polaron transformation. If the free excitations of the donor are delocalized, the displacements are matrices. As illustrated in Paper I,[7] the system and bath are entangled, which plays a crucial role in the subsequent dynamic evolution. To obtain the exact emission spectrum, one must account for the full system-bath correlations.

1. Perturbation expansion

In the below, we derive our new expression for the emission spectrum. As shown in Eq. (10), the system-bath coupling Hamiltonian H^D_{sb} appears in both the real- and imaginary-time domains. According to the previous analysis of the absorption spectrum,[7] it treats reliably the real-time evolution up to 2nd-order in H^D_{sb} as

$$\begin{aligned} e^{iH^D t} \simeq e^{iH^D_s t} e^{iH^D_b t}\Big\{1 + i\int_0^t ds\, H^D_{sb}(s) \\ - \int_0^t ds_2 \int_0^{s_2} ds_1 H^D_{sb}(s_2)\, H^D_{sb}(s_1)\Big\}, \end{aligned} \tag{16}$$

where $H^D_{sb}(s) = e^{i(H^D_s+H^D_b)s} H^D_{sb} e^{-i(H^D_s+H^D_b)s}$. Substituting the above equation into Eq. (10), we find

$$\mathbf{E}^D(t) \simeq e^{iH^D_s t}\sum_{n=0}^{2} i^n \mathcal{G}^{(n)}(t), \tag{17}$$

where

$$\begin{aligned} \mathcal{G}^{(0)} &= \mathrm{tr}_b \rho^D_e, \\ \mathcal{G}^{(1)}(t) &= \int_0^t ds\, \mathrm{tr}_b\left(H^D_{sb}(s)\,\rho^D_e\right), \\ \mathcal{G}^{(2)}(t) &= \int_0^t ds_2 \int_0^{s_2} ds_1 \mathrm{tr}_b\left[H^D_{sb}(s_2)\, H^D_{sb}(s_1)\,\rho^D_e\right]. \end{aligned} \tag{18}$$

Now we calculate the above three terms separately.

2. Zeroth-order term $\mathcal{G}^{(0)}$

The 0th-order term $\mathcal{G}^{(0)}$ is the RDM of the donor. Generally, ρ^D_e is not factorized and $\mathcal{G}^{(0)}$ could be far from the Boltzmann distribution for large system-bath coupling or low-temperature.[7]

In this paper, $\mathcal{G}^{(0)}$ is obtained by using the stochastic PI method, which is very efficient even for large realistic systems such as LH2, and thus

$$\mathcal{G}^{(0)} = \rho^D_{\mathrm{ex}}, \tag{19}$$

where ρ^D_{ex} is the exact RDM of the donor. Second-order corrections to the Boltzmann distribution are widely employed in many perturbative methods[7,10] by replacing t with $i\beta$ in Eq. (16). It is important to note that the expansion (16) is reliable for small t. The reason for its successful application in the absorption spectrum is that the population dynamics is not involved there, and the coherence usually decays in a very short time for large λ. If we replace the t with $i\beta$, the corrected RDM of the donor is equivalent to that obtained by letting $t \to \infty$ and is unreliable for large λ.

3. First-order term $\mathcal{G}^{(1)}(t)$

First of all, we should emphasize that although $\mathcal{G}^{(1)}(t)$ is the 1st-order term in the real-time expansion, it includes the effects of the system-bath equilibrium state on the dynamics to infinite order. After the following treatment of the imaginary-time effect, $\mathcal{G}^{(1)}(t)$ is 2nd-order in H^D_{sb}.

First, it is more convenient to write $\mathcal{G}^{(1)}(t)$ as

$$\mathcal{G}^{(1)}(t) = \int_0^t ds \sum_{m=1}^{N_D} V_m(s)\,\mathbf{B}_m(s), \tag{20}$$

where the operator

$$\mathbf{B}_m(s) = \mathrm{tr}_b\left(B_m(s)\,\rho^D_e\right) \tag{21}$$

is the displacement of the bath, which can be viewed as a generalized polaron shift. It has the same dimensionality as the system. This quantity plays an important role in the emission spectrum and accounts for the most significant difference between the emission and absorption spectra. This quantity is the average of the bath operator, it has not been widely recognized before, and it can be obtained exactly from the stochastic PI or the first level auxiliary fields of the HEOM.[14]

In traditional perturbative methods,[7,10] $\mathbf{B}_m(s)$ can be obtained by using the linear response theory, where the donor's operator V_m is treated as the external force, ρ^D_e is expanded in the imaginary-time domain and is kept up to the 1st-order of H^D_{sb}. Since the linear response theory works in the weak

coupling regime, the above treatment is reliable only when $|\beta H_s^D| \ll 1$, i.e., the thermal energy should be far larger than the energy gap of the donor's excitations.

In this work, as shown in Appendix A, we find

$$\mathbf{B}_m(s) \simeq -\Gamma(s)\{V_m, \rho_{\rm ex}^D\}, \tag{22}$$

where

$$\Gamma(s) = \int_0^\infty \frac{d\omega}{\pi}\frac{J(\omega)}{\omega}\cos(\omega s), \tag{23}$$

and $J(\omega)$ is the spectral density of the system-bath coupling. Equation (22) becomes exact if we trace the donor's degrees of freedom,

$$\langle B_m(s)\rangle = {\rm tr}_D[\mathbf{B}_m(s)] = -2\Gamma(s)\langle V_m\rangle. \tag{24}$$

Compared with Eq. (22), the traditional perturbative method[7] gives

$$\mathbf{B}_m(s) \simeq -\rho_{\rm eq}^D\int_0^\beta d\tau V(-i\tau)C_b(-s-i\tau), \tag{25}$$

where $\rho_{\rm eq}^D = \exp(-\beta H_s^D)/Z_{\rm eq}^D$ is the thermal state of the donor, and $C_b(z) \equiv {\rm tr}_b\left[e^{-\beta H_b^D}B(z)B(0)\right]/Z_b^D$ is the complex-time correlation function of the bath. Equation (22) can reduce to Eq. (25) in the high-temperature limit.

Substituting Eq. (22) into Eq. (20), we find

$$\mathcal{G}^{(1)}(t) \simeq -\int_0^t ds\,\Gamma(s)\sum_{m=1}^{N_D}V_m(s)\{V_m, \rho_{\rm ex}^D\}. \tag{26}$$

We can see that, although $\mathcal{G}^{(1)}(t)$ is the 1st-order term in the real-time expansion, it is actually a 2nd-order term in H_{sb}^D after the expansion of $\mathbf{B}_m(s)$. Eq. (26) is the central result in this work, and two points regarding to it should be emphasized.

(i) First, in the high-temperature limit, both the above treatment of $\mathbf{B}_m(t)$ and other perturbative methods such as the FCE[7,10] will go to the same limit. The difference is that, in traditional perturbative treatments, $\mathbf{B}_m(s)$ is expanded in terms of H_{sb}^D, while $H_s^D + H_b^D$ is left to be the free Hamiltonian. Hence the density matrices of the donor and bath are Boltzmann distributions, which deviate from the exact distributions with the increase of λ and β, especially when the donor's free excitation is delocalized. This type of expansion was found to be very unstable when $|\beta H_s^D| > 1$[7] even for the lowest order term $H_{sb}^D(s-i\tau)$.

In our new approach, the total Hamiltonian H^D is treated as the free part, and $\mathbf{B}_m(s)$ is expanded in terms of the commutator $[H^D, B_m(s)] \sim B_m(s)$. In this case, the influence of the bath on the system is explicitly included in the exact RDM $\rho_{\rm ex}^D$. Therefore, the leading term of the new expansion is much more accurate, and the expansion converges faster than the traditional perturbative treatments. As shown in our Paper IV,[6] only with the above treatment, we can give a reliable estimate of the emission spectrum and MCFT rate for the LH2 complex.

(ii) As we analyzed above, the displacement of the bath should be a scalar if the donor's excitation is fully localized. In this case, $\rho_{\rm ex}^D$ is diagonal in the site basis, and thus

$$V_m\rho_{\rm ex}^D = \rho_{\rm ex}^D V_m = p_m^D V_m, \tag{27}$$

where p_m^D is the population of the mth site. Therefore,

$$\mathbf{B}_m(s) = -2\Gamma(s)p_m^D V_m. \tag{28}$$

Although the above $\mathbf{B}_m(s)$ is a matrix, it has only one non-zero element, meaning that $\mathbf{B}_m(s)$ is effectively a scalar. The displacement of the bath that is coupled to the mth site is irrelevant to the other sites. If the donor's excitations are delocalized, $\rho_{\rm ex}^D$ is not a diagonal matrix any more, and the displacement $\mathbf{B}_m(s)$ is a matrix. In this case, the displacement of the bath is determined not only by a single site, but also by all the others.

4. Second-order term $\mathcal{G}^{(2)}(t)$

In traditional perturbation treatments, the density matrix used in $\mathcal{G}^{(2)}(t)$ is factorized $\rho_e^D \simeq \rho_{\rm eq}^D\rho_b^D$, which is the lowest order expansion of ρ_e^D with respect to the system-bath coupling H_{sb}^D. Here, $\rho_{\rm eq}^D$ and ρ_b^D are the respective Boltzmann distributions of the free Hamiltonian H_s^D and H_b^D. Therefore, the influence of the bath on the system is totally ignored. Actually, we can also expand the equilibrium state ρ_e^D as

$$\rho_e^D = \rho_{\rm ex}^D\rho_b^D + \varrho_{\rm sb}, \tag{29}$$

where ${\rm tr}_b\varrho_{\rm sb} = 0$. In the above expansion, the influence of the bath on the equilibrium properties of the system is included explicitly in $\rho_{\rm ex}^D$. The influence of the system on the bath as well as their correlations $\varrho_{\rm sb}$ can be neglected in $\mathcal{G}^{(2)}(t)$, since it will induce complex-time correlations that go beyond the second-order of H_{sb}^D. Therefore, we obtain

$$\mathcal{G}^{(2)}(t) = \int_0^t ds_2\int_0^{s_2} ds_1 C_b(s_2-s_1) \times\sum_{m=1}^{N_D}V_m(s_2)V_m(s_1)\rho_{\rm ex}^D. \tag{30}$$

One may notice the different treatments of ρ_e^D in $\mathcal{G}^{(1)}(t)$ and $\mathcal{G}^{(2)}(t)$. In the calculation of $\mathcal{G}^{(2)}(t)$, the displacement of the system on the bath is included in $\varrho_{\rm sb}$. However, this displacement happens in the initial equilibrium state, i.e., the imaginary-time domain. We neglect this term since our expansion truncates at second-order. Actually, $\varrho_{\rm sb}$ is a mixture of the system bath interactions, and it is quite difficult to derive its explicit form. Nevertheless, the lowest order term of $\varrho_{\rm sb}$ can be inferred from the calculation of $\varrho_{\rm sb}$. In summary, up to the 2nd-order of H_{sb}^D, the above calculations are self consistent.

5. Second-order hybrid cumulant expansion

Now, we can write Eq. (17) in a cumulant expansion form as

$$\mathbf{E}^D(t) = \exp(iH_s^D t)\exp[\mathcal{K}^{RR}(t) + \mathcal{K}^{RI}(t)]\rho_{\rm ex}^D, \tag{31}$$

where the matrices

$$\mathcal{K}^{RR}(t) = -\sum_{m=1}^{N_D}\int_0^t ds_2\int_0^{s_2} ds_1 \times C_b(s_2-s_1)V_m(s_2)V_m(s_1) \tag{32}$$

and

$$\mathcal{K}^{RI}(t) = -i\sum_{m=1}^{N_D}\int_0^t ds\,\Gamma(s) \times V_m(s)\left[V_m + \rho_{\rm ex}^D V_m \left(\rho_{\rm ex}^D\right)^{-1}\right]. \quad (33)$$

Since the exact RDM is obtained numerically from stochastic PI, we can regard the new method as a 2nd-order hybrid cumulant expansion (HCE). In fact, both the HCE and FCE[7] will tend to the same limit when the temperature T goes to infinity. In this case, the correlations between the donor and its bath disappears, $\rho_e^D = \rho_{ex}^D \rho_b^D$. Moreover, since $\beta = 1/k_B T \to 0$, we have $\rho_{ex}^D \to \mathbb{I}/N^D$, where $\mathbb{I}$ is the identity matrix of the donor.

III. NUMERICAL COMPARISONS

A. Case I: Two-level systems

Below, we shall compare the HCE method (31) with the exact stochastic PI[5] and FCE[7] methods. In this case, we consider a two-level system, of which the free Hamiltonian is

$$H_s^D = \begin{pmatrix} 0 & V \\ V & 0 \end{pmatrix}. \quad (34)$$

This model Hamiltonian was used in our Paper I[7] to show the reliability of the FCE method. The free excitations of this donor are fully delocalized, and the energy gap of the excitations is $2V$. In the following calculations, the temperature is $T = 300$ K, and the system-bath coupling spectrum takes the Drude form

$$J(\omega) = \frac{2\lambda\omega\gamma}{\omega^2+\gamma^2}, \quad (35)$$

where λ is the reorganization energy, and the cutoff frequency of the bath is $\gamma = 10\ \mathrm{ps}^{-1}$. These parameters are comparable to the real LH2 system. The coupling between the donor and the acceptor is set to be $J_{mn} = J$; therefore, the emission spectrum tensor in the MCFT rate for this system is given by Eq. (15).

In the first example, we set $V = 50\ \mathrm{cm}^{-1}$, which is smaller than the thermal energy at $T = 300$ K, and $|\beta H_s^D| \sim 0.5$ lies in the safe regime for both the FCE and HCE methods. Numerical results are shown in Fig. 1. We see that, when $\lambda = 100\ \mathrm{cm}^{-1}$, both perturbative methods give very accurate results. Even for $\lambda = 500\ \mathrm{cm}^{-1}$, the perturbative results are very close to the exact one, which is obtained by using the PI. When $\lambda = 1000\ \mathrm{cm}^{-1}$, which is far larger than any other energy scales, the position and width of the emission spectrum given by the FCE method is no longer accurate as compared with the HCE method, which is still reliable.

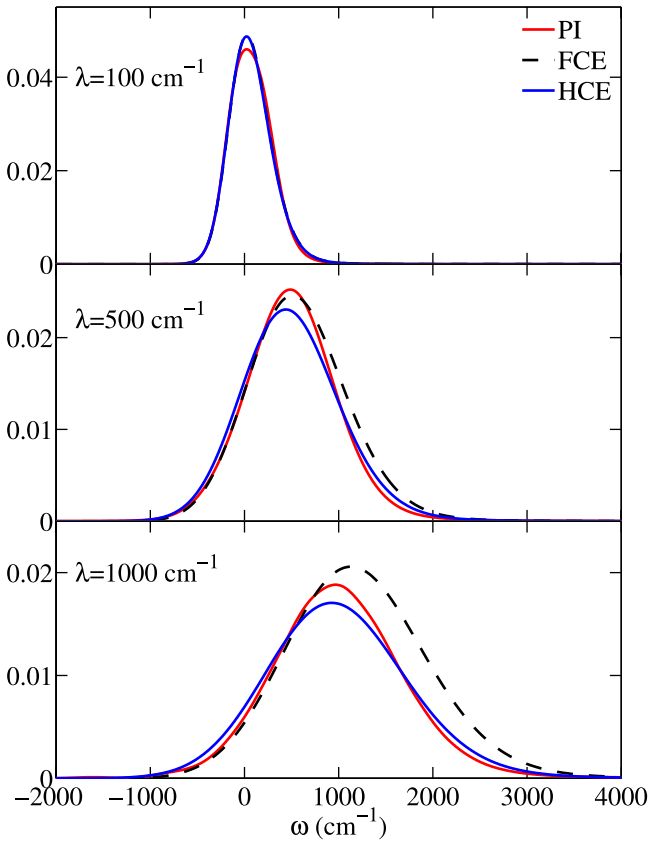

FIG. 1. Emission spectrum (15) of the model system in Case I with $V = 50\ \mathrm{cm}^{-1}$. The cutoff frequency of the bath is $\gamma = 10\ \mathrm{ps}^{-1}$ and the temperature is $T = 300$ K. The thermal energy is larger than the energy gap of the system's excitations, and both the FCE and HCE methods are reliable even when $\lambda = 500\ \mathrm{cm}^{-1}$. For very large reorganization energy $\lambda = 1000\ \mathrm{cm}^{-1}$, the HCE remains accurate while the spectrum given by the FCE deviates consistently from the exact result.

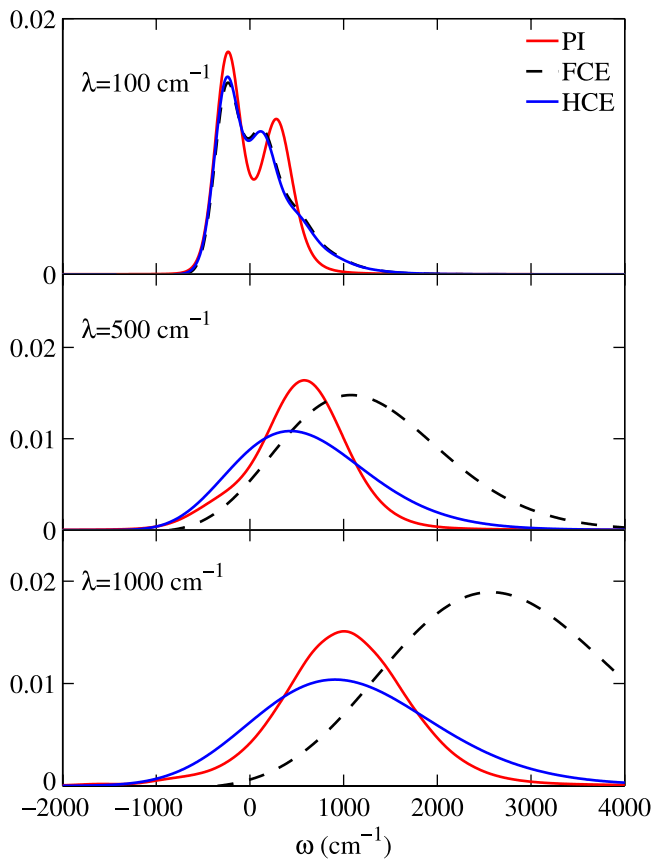

FIG. 2. Emission spectrum (15) of the system in Case I with $V = 200\ \mathrm{cm}^{-1}$. The other parameters are the same as in Fig. 1. In this case, the thermal energy is smaller than the energy gap of the system's excitations, which is actually out of the working regime of the perturbative methods. However, the HCE can still give physically reasonable spectrum.

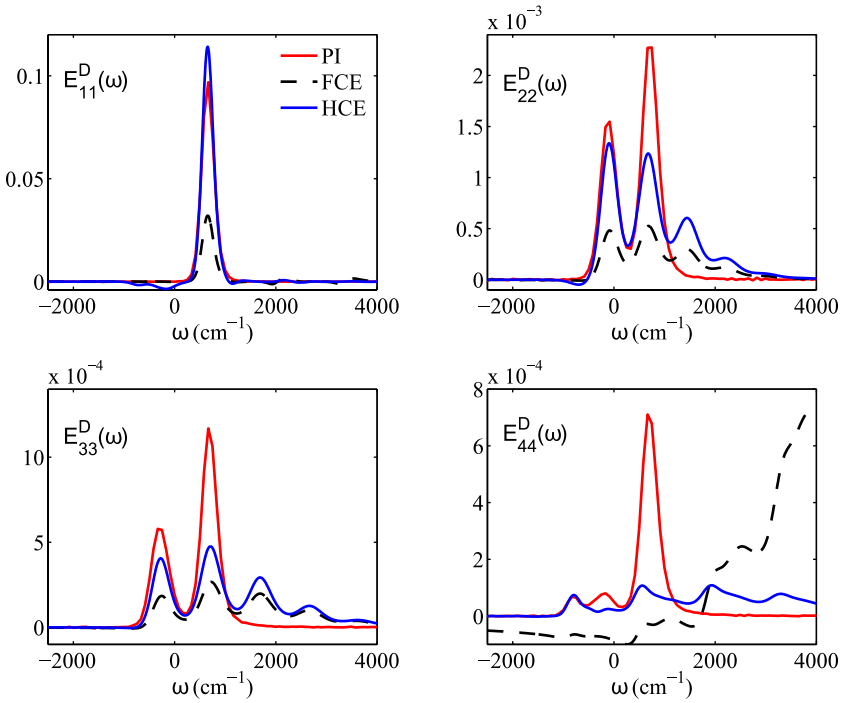

FIG. 3. Emission spectra of the four-level system (Case II) in the exciton basis $\mu = 1, 2, 3, 4$. Here, we only focus on the diagonal terms of $\mathbf{E}^D(\omega)$ for $\lambda = 160$ cm^{-1}, $T = 300$ K, and $\gamma = 10$ ps^{-1}. For the lowest excitation level, the HCE method gives almost the same result as the exact stochastic PI method. The spectrum given by the FCE method is far from the exact one. For higher excitations, both perturbative results deviate from the exact one, however, the HCE method is much more reliable than the FCE method. The exact results are obtained by our recently developed stochastic PI method,[5] and it is difficult to achieve a converged spectrum from the HEOM method since the donor's excitation energies are much higher than the thermal energy.

Now, we increase the energy gap of the excitation to 400 cm^{-1}, i.e., $V = 200$ cm^{-1}. In this case, $|\beta H_s^D| \sim 2$ is beyond the perturbation regime. As shown in Fig. 2, the FCE and HCE methods give similar results for $\lambda = 100$ cm^{-1}, which slightly deviates from the exact spectrum. When the reorganization energy increases to 500 cm^{-1} and 1000 cm^{-1}, the width and peak shift are so far from the exact result that the spectrum obtained by the FCE method tends to be divergent. The spectrum obtained by the HCE method is much closer to the exact results. Although the width of the spectrum is slightly wider than the exact one, the shift of the peak is correct, which means the treatment of the displacement (22) is more precise.

B. Case II: Four-level system

A systematic comparison of different methods for the LH2 complex will be presented in our Paper IV,[6] where the benchmark emission spectrum and MCFT rate are obtained by our stochastic PI method. Here, for the sake of simplicity, we adopt a smaller system. The LH2 complex consists of 18 chromophores, which forms a dimerized ring that has nine-fold symmetry. We select four adjacent chromophores from the LH2 system and construct a smaller ring. Although the new system is much smaller, it captures some key factors of the LH2 complex. The Hamiltonian of the four-site system is (in the unit of cm^{-1})

$$H_s^D = \begin{pmatrix} 0 & 360 & -100 & 320 \\ 360 & 190 & 320 & -100 \\ -100 & 320 & 0 & 360 \\ 320 & -100 & 360 & 190 \end{pmatrix}, \tag{36}$$

where the site energies are shifted to the lowest one. For the above system, the largest energy gap of the excitations is much larger then the thermal energy at $T = 300$ K, and $|\beta H_s^D|_{\max} \sim 6.6$. We note that, for multi-chromophoric systems, the donor-acceptor couplings J_{mn} are not identical. Therefore, the MCFT rate cannot be simplified to (14). In the LH2 systems, we focus on the MCFT rate between two LH2 rings. Due to the specific form of the dipole-dipole couplings, the MCFT rate is mainly determined by the lower excitations. In Fig. 3, we select the diagonal matrix elements of $\mathbf{E}^D(\omega)$ in the exciton basis to compare the results of different methods. The FCE method fails to give reliable spectra, and thus cannot be applied to calculate the MCFT rate of LH2. The HCE method is quite reliable. For the lowest three levels, the emission spectra are in good agreement with the exact results. The highest excitation is far from the high-temperature approximation, so it is very hard to get a converged emission spectrum for this system even with the HEOM method. The results of the four-level system help us to understand the performance of the FCE and HCE in the real LH2 system as shown in our Paper IV.[6]

IV. CONCLUSION

We develop a HCE method to calculate the emission spectrum and MCFT rate. Traditional perturbative methods such as the second-order full cumulant expansion and the time-convolutionless master equation are problematic when the system's excitations are delocalized and the energy gap of the excitations are comparable to or larger than the thermal energy. In this case, the polaron displacements in the bath are matrices, not scalars, and the exact statistics of the bath are far from the Boltzmann distribution of the free bath. However, in these perturbative methods, the total equilibrium state is expanded with respect to the system-bath coupling term, which is subsequently averaged over the unperturbed Boltzmann bath. This is the fundamental reason that such perturbative or

cumulant expansion treatments can give reliable absorption spectra but not emission spectra.

In this paper, the bath displacement operator $\mathbf{B}_m(t)$ is expanded with respect to the commutators $[H^D, B_m] \sim B_m$ but not the system-bath coupling H^D_{sb}. The influence of the bath on the system is described by the exact reduced density matrix of the system, which can be obtained readily from the stochastic path integral method.[15] The reliability of the hybrid cumulant method is verified by using a delocalized two-level system and a delocalized four-level system similar to the LH2 complex. When the thermal energy is larger than the energy gap of the excitations, both the hybrid cumulant and the second-order full cumulant[7] methods give reliable emission spectra, but the hybrid cumulant expansion method performs significantly better for large system-bath coupling. When the thermal energy is smaller than the energy gap of the excitations, only the hybrid cumulant expansion method gives reliable emission spectra. The application of the hybrid cumulant expansion method in the MCFT rate of the LH2 complex will be given in our Paper IV,[6] where different perturbative methods are calibrated with our newly developed stochastic path integrals.

Note added in proof. Computer codes for stochastic simulations of absorption spectra, emission spectra, and Forster rates are available for download at http://web.mit.edu/jianshucaogroup/resources.html.

APPENDIX A: DERIVATION OF $B_m(s)$

In this section, we calculate

$$\mathbf{B}_m(s) \equiv \mathrm{tr}_b\left(B_m(s)\,\rho_e^D\right).$$

First, it is straightforward to show that

$$\langle B_m(s)\rangle = \mathrm{tr}_D\left[\mathbf{B}_m(s)\right] = -\frac{1}{\beta}\left(\frac{d}{d\epsilon}\right)_{\epsilon=0} \ln Z_e^D(\epsilon), \tag{A1}$$

where

$$Z_e^D(\epsilon) = \mathrm{tr} e^{-\beta\left(H^D+\epsilon B_m(s)\right)} \tag{A2}$$

is the partition function of the perturbed Hamiltonian. As proved in Appendix B, the above partition function can be expressed as

$$Z_e^D(\epsilon) = \mathrm{tr} e^{-\beta\left[H^D-2\epsilon\Gamma(s)V_m-\epsilon^2\lambda\right]}, \tag{A3}$$

where

$$\Gamma(t) = \int_0^\infty \frac{d\omega}{\pi}\frac{J(\omega)}{\omega}\cos(\omega t), \tag{A4}$$

and $J(\omega)$ is the spectral density of the system-bath coupling. Therefore, we find

$$\langle B_m(s)\rangle = -2\Gamma(s)\langle V_m\rangle, \tag{A5}$$

where $\langle V_m\rangle = \mathrm{tr}_D\left(V_m\rho_{\mathrm{ex}}^D\right)$. The relationship between the above result and the linear response theory will be studied in our further work. In the monomer case, this above result becomes $\langle B(s)\rangle = -2\Gamma(s)$.

To calculate $\mathcal{G}^{(1)}(t)$, what we need is $\mathbf{B}_m(s)$ but not $\langle B_m(s)\rangle$, and the above derivation is exact if we remove the trace of the donor's degrees of freedom. Inspired by the above analysis, we consider the following quantity:

$$\tilde{B}_m(s) \equiv -\frac{1}{\beta Z_e^D}\left(\frac{d}{d\epsilon}\right)_{\epsilon=0} \mathrm{tr}_b e^{-\beta\left[H^D+\epsilon B_m(s)\right]}, \tag{A6}$$

which can be expanded systematically by using the formula

$$\left(\frac{d}{d\epsilon}\right)_{\epsilon=0} e^{-\beta\left[H^D+\epsilon B_m(s)\right]} = -e^{-\beta H^D}\sum_{n=0}^{\infty}\frac{\left(\beta\mathcal{L}^D\right)^n}{(n+1)!}B_m(s), \tag{A7}$$

where $\mathcal{L}^D \equiv [H^D, .]$. It is easy to show that if we trace the degrees of freedom of both the donor and bath, the above equation is nonzero only for $n = 0$, this actually gives Eq. (A1). Now, if we trace the degrees of freedom of the bath only, the first three terms of Eq. (A6) become

$$\tilde{B}_m(s) \simeq \mathbf{B}_m(s) + \frac{\beta}{2}\mathrm{tr}_b\left(\rho_e^D\left[H^D, B_m(s)\right]\right) + \frac{\beta^2}{6}\mathrm{tr}_b\left(\rho_e^D\left[H^D,\left[H^D, B_m(s)\right]\right]\right). \tag{A8}$$

Since $\left[H^D, B_m(s)\right] \sim B_m(s) \sim \lambda$, we see

$$\mathbf{B}_m(s) = \tilde{B}_m(s) + O(\beta\lambda). \tag{A9}$$

When $s = 0$, it is easy to find $\mathrm{tr}_b\left(\rho_e^D\left[H^D, B_m\right]\right) = 0$, and then

$$\mathbf{B}_m = \tilde{B}_m + O\left[(\beta\lambda)^2\right]. \tag{A10}$$

In the high-temperature limit, $\tilde{B}_m = \mathbf{B}_m$. The next step is to calculate $\tilde{B}_m(s)$. As shown in Appendix B, with the polaron transformation we find

$$\tilde{B}_m(s) = -\frac{1}{\beta Z_e^D}\left(\frac{d}{d\epsilon}\right)_{\epsilon=0} \mathrm{tr}_b e^{-\beta\left[H^D-\epsilon 2\Gamma(s)V_m\right]}. \tag{A11}$$

Using the same expansion as Eq. (A8), we find

$$\tilde{B}_m(s) = -\Gamma(s)\left\{V_m, \rho_{\mathrm{ex}}^D\right\} + O\left(\beta H_s^D\right), \tag{A12}$$

where $\{A, B\} \equiv AB + BA$. The above expression is symmetrized to ensure $\tilde{B}_m(s)$ is Hermitian.

Finally, we arrive at the explicit expression of the displacement of the bath

$$\mathbf{B}_m(s) \simeq -\Gamma(s)\left\{V_m, \rho_{\mathrm{ex}}^D\right\}. \tag{A13}$$

APPENDIX B: DERIVATION OF EQ. (A11)

To derive Eq. (A11), we need to show the following relation:

$$\mathrm{tr}_b e^{-\beta\left[H^D+\epsilon B_m(s)\right]} = \mathrm{tr}_b e^{-\beta\left[H^D-\epsilon 2\Gamma(s)V_m-\epsilon^2\lambda\right]}. \tag{B1}$$

We shall use the polaron transformation

$$D_m(\epsilon,t) \equiv \exp\left[-\epsilon\sum_k \frac{g_{m,k}}{\omega_{m,k}}\left(b_{m,k}^\dagger e^{-i\omega_{m,k}t} - b_{m,k}e^{i\omega_{m,k}t}\right)\right], \tag{B2}$$

which can be expressed as

$$D_m(\epsilon,t) = U_m(t)\,D_m(\epsilon,0)\,U_m^\dagger(t), \tag{B3}$$

where

$$U_m(t) = \exp\left(-i\sum_k \omega_{m,k} b^\dagger_{m,k} b_{m,k}\right). \quad \text{(B4)}$$

Since

$$D_m(\epsilon,0)\, b_{m,k} D^\dagger_m(0) = b_{m,k} + \epsilon \frac{g_{m,k}}{\omega_{m,k}}, \quad \text{(B5)}$$

we have

$$D_m(\epsilon,t)\, b_{m,k} D^\dagger_m(\epsilon,t) = b_{m,k} + \epsilon \frac{g_{m,k}}{\omega_{m,k}} e^{i\omega_{m,k}t}. \quad \text{(B6)}$$

Therefore,

$$\begin{aligned} &D_m(\epsilon,t)\, H^D D^\dagger_m(\epsilon,t) \\ &\quad = H^D + \epsilon \mathbb{I}_D \otimes B_m(t) + 2\epsilon V_m \Gamma(t) + \epsilon^2\lambda, \end{aligned} \quad \text{(B7)}$$

where

$$\begin{aligned} \Gamma(t) &\equiv \sum_k \frac{g^2_{m,k}}{\omega_{m,k}} \cos(\omega_{m,k}t) \\ &= \int_0^\infty \frac{d\omega}{\pi} \frac{J(\omega)}{\omega} \cos(\omega t). \end{aligned} \quad \text{(B8)}$$

If $J(\omega)$ is the Drude spectrum (35), $\Gamma(t) = \lambda e^{-\gamma t}$. From Eq. (B7), we find

$$\begin{aligned} &H^D + \epsilon \mathbb{I}_D \otimes B_m(t) \\ &\quad = D_m(\epsilon,t)\, H^D D^\dagger_m(\epsilon,t) - 2\epsilon V_m \Gamma(t) - \epsilon^2\lambda \\ &\quad = D_m(\epsilon,t)\left[H^D - 2\epsilon V_m \Gamma(t) - \epsilon^2\lambda\right] D^\dagger_m(\epsilon,t), \end{aligned}$$

and thus

$$\begin{aligned} &\mathrm{tr}_b e^{-\beta\left[H^D + \epsilon B_m(s)\right]} \\ &\quad = \mathrm{tr}_b D_m(\epsilon,s)\, e^{-\beta\left[H^D - 2\epsilon\Gamma(t)V_m - \epsilon^2\lambda\right]} D^\dagger_m(\epsilon,s) \\ &\quad = \mathrm{tr}_b e^{-\beta\left[H^D - 2\epsilon\Gamma(t)V_m - \epsilon^2\lambda\right]}. \end{aligned} \quad \text{(B9)}$$

The 2nd-order term $\epsilon^2\lambda$ has no effect after the derivative $(d/d\epsilon)_{\epsilon=0}$, and Eq. (A11) is obtained.

[1] T. Förster, in *Modern Quantum Chemistry*, edited by O. Sinanoglu (Academic Press, New York, 1965), Vol. 3.
[2] H. Sumi, J. Phys. Chem. B **103**, 252 (1999).
[3] J. Strümpfer and K. Schulten, J. Chem. Phys. **134**, 095102 (2011).
[4] Y. Jing, L. Chen, S. Bai, and Q. Shi, J. Chem. Phys. **138**, 045101 (2013).
[5] J. Moix, J. Ma, and J. Cao, "Förster resonance energy transfer, absorption and emission spectra in multichromophoric systems. III. Exact stochastic path integral evaluation," J. Chem. Phys. **142**, 094108 (2015).
[6] J. Ma, J. Moix, and J. Cao, "Exact evaluation of the energy transfer rates and steady state absorption and emission spectra in the b850 photosynthetic complexes of LH2" (unpublished).
[7] J. Ma and J. Cao, "Förster resonance energy transfer, absorption and emission spectra in multichromophoric systems. I. Full cumulant expansions and system-bath entanglement," J. Chem. Phys. **142**, 094106 (2015).
[8] S. Mukamel, *Principles of Nonlinear Optical Spectroscopy* (Oxford University Press, 1995).
[9] T. Renger and R. A. Marcus, J. Chem. Phys. **116**, 9997 (2002).
[10] L. Banchi, G. Costagliola, A. Ishizaki, and P. Giorda, J. Chem. Phys. **138**, 184107 (2013).
[11] S. Maier, T. L. Schmidt, and A. Komnik, Phys. Rev. B **83**, 085401 (2011).
[12] C. K. Lee, J. Moix, and J. Cao, J. Chem. Phys. **136**, 204120 (2012).
[13] L. Cleary and J. Cao, New J. Phys. **15**, 125030 (2013).
[14] L. Zhu, H. Liu, W. Xie, and Q. Shi, J. Chem. Phys. **137**, 194106 (2012).
[15] J. M. Moix, Y. Zhao, and J. Cao, Phys. Rev. B **85**, 115412 (2012).